Excess Centrosomes Disrupt Vascular Lumenization and Endothelial Cell Adherens Junctions

Danielle M Berlin[a], Erich J Kushner[b], Katy L Davis[b], and Victoria L Bautch[a,b,c,#]

[a]Curriculum in Cell Biology and Physiology, The University of North Carolina at Chapel Hill, Chapel Hill, North Carolina 27599, USA.
[b]Department of Biology, The University of North Carolina at Chapel Hill, Chapel Hill, North Carolina 27599, USA.
[c]McAllister Heart Institute, The University of North Carolina at Chapel Hill, Chapel Hill, North Carolina 27599, USA.

[#]Corresponding author: Victoria L Bautch, PhD
Professor of Biology
Department of Biology, CB#3280
University of North Carolina at Chapel Hill
Chapel Hill, NC 27599 USA
Phone: 919-966-6797

E-mail: bautch@med.unc.edu

Running head: CENTROSOMES IN VASCULAR LUMENIZATION AND JUNCTIONS

WORKING TITLE: 10 words
Abstract: 146 words
Text: 4,397 words
Figures: 4

ABSTRACT

Proper blood vessel formation requires coordinated changes in endothelial cell polarity and rearrangement of cell-cell junctions to form a functional lumen. One important regulator of cell polarity is the centrosome, which acts as a microtubule organizing center. Excess centrosomes perturb aspects of endothelial cell polarity linked to migration, but whether centrosome number influences apical-basal polarity and cell-cell junctions is unknown. Here, we show that excess centrosomes alter the apical-basal polarity of endothelial cells in angiogenic sprouts and disrupt endothelial cell-cell adherens junctions. Endothelial cells with excess centrosomes had narrower lumens in a 3D sprouting angiogenesis model, and zebrafish intersegmental vessels had reduced perfusion following centrosome overduplication. These results indicate that endothelial cell centrosome number regulates proper lumenization downstream of effects on apical-basal polarity and cell-cell junctions. Endothelial cells with excess centrosomes are prevalent in tumor vessels, suggesting how centrosomes contribute to the dysfunction of tumor vasculature.

Keywords: Endothelial cell, centrosome, junctions, polarity, lumen, angiogenesis

66 **INTRODUCTION**

67 Angiogenesis is the sprouting of new blood vessels from pre-existing
68 vasculature, and it is crucial during development, pregnancy, wound healing, and
69 tumorigenesis [1–3]. Endothelial cells (EC) form new sprouts that then extend,
70 lumenize, and connect with other sprouts and vessels to provide new conduits for blood
71 flow and create a functional vascular network. This process requires dynamic
72 rearrangement of endothelial cell-cell junctions and establishment of apical-basal
73 polarity, such that the apical surface of EC faces the vessel lumen and the basal
74 surface faces the tissue [4–8]. Lumen formation closely follows sprout formation and
75 extension temporally, and many sprout tips have two or more EC that are polarized in
76 the apical-basal axis [9]. However, it is not known how centrosome number contributes
77 to this process.

78

79 As tumors grow, hypoxia leads to elevated levels of pro-angiogenic factors such
80 as vascular endothelial growth factor (VEGF-A) that promote neo-angiogenesis to
81 vascularize the tumor. However, the blood vessels surrounding these tumors are often
82 leaky, tortuous, and not properly lumenized [10–12], suggesting defects in EC junctions
83 and polarity. Interestingly, tumor vessels are also characterized by EC with excess
84 centrosomes [13,14]. High VEGF-A signaling in EC results in centrosome
85 overduplication, which affects interphase cells by increasing invasiveness, elevating
86 microtubule (MT) nucleations, changing aspects of polarity and migration, and altering
87 signaling dynamics [13,15–17]. However, it is unclear how excess centrosomes impact

88 cell-cell interactions and lumenogenesis, which require proper cytoskeletal dynamics
89 [18,19].
90
91 Cadherins form cell-cell adherens junctions that link to the actin cytoskeleton and
92 restrict the apical vs. basolateral domains in epithelial cells [20,21]. In EC, VE-cadherin
93 is the primary component of the vascular adherens junction and is required for
94 localization of apical markers during lumen formation in zebrafish intersegmental
95 vessels (ISVs) [7]. Depletion of VE-cadherin is embryonically lethal in zebrafish and
96 mice due to severe vascular defects, including a lack of vascular lumens [22,23]. The
97 centrosome acts as a major microtubule organizing center and determinant of cell
98 polarity [24,25]. As EC sprout and lumenize, they are not columnar, but flattened in the
99 apical-basal plane. Although more filamentous actin appears on the apical side of EC
100 [26–28], the topology of the centrosome is not well-defined, and the effects of
101 centrosome perturbation on apical-basal polarity have not been investigated.
102
103 Here, we show for the first time that excess centrosomes prevent the proper
104 polarization of interacting EC. Excess centrosomes resulted in EC with destabilized
105 adherens junctions and narrow and closed vascular lumens both *in vitro* and *in vivo*.
106 These findings reveal a novel role for the centrosome in EC apical-basal polarity, and in
107 junction and lumen formation, and suggest how excess centrosomes in the vasculature
108 may contribute to poor perfusion in tumor vessels.

RESULTS

Excess centrosomes perturb polarization of junctionally linked EC

We previously showed that excess centrosomes interfere with repolarization along the forward-rearward axis in sprouting EC [15], and thus we hypothesized that supernumerary centrosomes disrupt multiple EC polarity axes. We examined the polarity between EC sharing junctions using an inducible system to overexpress polo-like kinase 4 (Plk4) in human umbilical vein endothelial cells (HUVEC) **(Fig. 1a)**. Plk4 regulates centriole duplication, and its overexpression downstream of a TRE (tet-responsive element) upon addition of doxycycline (DOX) results in supernumerary centrosomes [13,15,29,30]. HUVEC were seeded onto H-shaped micropatterns that allow for polarity assessment between two EC that form a cell-cell junction. Polarity was defined based on centrosome position relative to the nucleus and cell-cell junction, with a “proximal” position being near the cell-cell junction, a “central” position in the nuclear region, and a “distal” position between the nucleus and the cell periphery **(Fig. 1b)**. EC with a normal centrosome number (1-2) typically had a distal centrosome polarity (**Fig. 1c-d**). In contrast, EC with excess centrosomes (>2) showed a significant increase in centrosome proximal polarity, indicating that centrosome number affects EC polarization relative to cell-cell junctions **(Fig. 1c-d)**. Interestingly, when two EC with normal centrosome number (N:N) formed a junction, both cells usually had centrosomes in the distal position, which we termed “normal” polarity **(Fig. 1e)**. All other polarity combinations were deemed abnormal. When both EC forming a junction had excess centrosomes (O:O), polarity was randomized between normal and abnormal **(Fig. 1e)**. Furthermore, N:N EC combinations were more likely to have cells with matching

132 polarity, while EC with an O:O combination were less likely to have the same polarity as
133 their neighbor **(Fig. 1f).** Taken together, these data indicate that excess centrosomes
134 prevent proper polarization of EC relative to cell-cell junctions.
135
136 ***EC with excess centrosomes form disorganized adherens junctions***
137 Because interacting EC with excess centrosomes had perturbed polarity in the
138 junction axis, we asked whether EC cell-cell interactions were influenced by centrosome
139 number. Adherens junctions are required for proper apical-basal polarity in epithelial
140 cells [7,31], and the distribution of VE-cadherin at EC adherens junctions is indicative of
141 junction maturity; a linear VE-cadherin pattern is associated with mature stabilized
142 junctions, while a serrated and punctate VE-cadherin pattern is associated with
143 activated and/or disrupted junctions [32]. To determine how excess centrosomes
144 influence adherens junctions, we seeded induced tet-Plk4 HUVEC onto H-shaped
145 micropatterns. Due to the heterogeneous nature of Plk4-induced centrosome over-
146 duplication a given cell-cell junction could have contributions from two EC with a normal
147 number of centrosomes (N:N), two EC with excess centrosomes (O:O), or one of each
148 (N:O) **(Fig. 2a-a")**. We found that junctions with contributions from EC with normal
149 centrosome numbers had more linear and stable junctions, while junctions with
150 contributions from EC with excess centrosomes formed more chaotic and disrupted
151 junctions **(Fig. 2b-b", c-c")**. These chaotic junctions had an increase in the total area of
152 VE-cadherin **(Fig. 2d)**, and line scans across the junctions revealed a more dispersed
153 VE-cadherin distribution when one or both EC had excess centrosomes **(Fig. 2e)**.

154 Overall, these findings indicate that EC with excess centrosomes do not maintain proper
155 endothelial cell-cell adherens junctions.
156
157 ***EC with excess centrosomes have abnormal lumens***
158 We hypothesized that the disrupted polarity seen between EC with
159 supernumerary centrosomes had physiological consequences. To examine apical-
160 basal polarity in EC, we used a 3D sprouting angiogenesis assay in which lumenized
161 sprouts form that appropriately polarize in the apical-basal axis [9,33]. We analyzed
162 sprouts formed from DOX-treated tet-Plk4 HUVEC expressing centrin::eGFP and
163 stained for Moesin1 as an apical marker **(Fig. 3a-b)** and found that EC with normal
164 centrosome numbers (1-2) typically had apically positioned centrosomes, while EC with
165 excess centrosomes (>2) had randomized centrosome polarity in the apical-basal axis
166 **(Fig. 3b-c)**. In addition, EC with excess centrosomes were more likely to have punctate
167 Moesin1, basal Moesin1, or unpolarized abnormal Moesin1 staining patterns compared
168 to normal linear and apical patterns **(Fig. 3b, d)**, indicative of polarity defects.
169
170 Since both apical-basal polarity and proper junction formation are important for
171 lumen formation [4–8], we hypothesized that excess centrosomes in EC perturb vessel
172 lumenogenesis. To normalize for overall vessel structure, we measured the width of the
173 vessel lumen relative to the total vessel width. We found that EC with excess
174 centrosomes had narrower lumens compared to EC with normal centrosome numbers
175 in 3D sprouts **(Fig 3b, e)**. Interestingly, there were several examples where lumens
176 were completely closed around EC with supernumerary centrosomes. These findings

177 indicate that EC centrosome number regulates proper vessel lumen diameter, likely
178 through effects on apical-basal polarity.
179
180 ***Overexpression of Plk4 in zebrafish results in fewer lumenized vessels***
181 To determine if centrosome number affects lumen formation *in vivo*, we fused a
182 *p2a-loxP-mCherry-STOP-loxP-Plk4* transgene to the 3' end of the endogenous *kdrl*
183 gene for vascular-selective expression of Plk4 after loxP site excision **(Fig. 4a)**. Adult
184 fish were then crossed to a *Tg(fli:centrin-GFP)* line, which allowed for visualization of
185 EC centrosomes. F1 embryos were injected with Cre mRNA and *Plk4* overexpression
186 was determined by loss of the mCherry signal. Fish with *Plk4* overexpression had an
187 increase in the percentage of EC with >2 centrosomes **(Fig. 4b-c)**. To determine if
188 overexpression of *Plk4* affected lumenogenesis, we performed microangiography at 72
189 hpf by injecting fluorescent microcarrier beads into the fish vasculature and examining
190 the intersegmental vessels (ISVs) for patency. Embryos with *Plk4* overexpression had
191 fewer perfused ISVs compared to wild type controls or fish lacking Cre **(Fig. 4d-e)**.
192 Reduced perfusion is indicative of narrower or absent lumens, suggesting that excess
193 centrosomes induced by *Plk4* overexpression lead to disrupted lumenogenesis *in vivo*.

194 **DISCUSSION**

195 Angiogenesis involves migration and rearrangement of EC, and leads to new
196 conduits through anastomosis and lumen formation between adjacent EC [1–3]. It is
197 clear that cell-cell interactions and polarization in several axes are important for lumen
198 formation, but the role of the centrosome in these processes is poorly understood. Here,
199 we show that supernumerary centrosomes perturb EC polarity and cell adhesion and
200 disturb lumen formation *in vitro* and *in vivo*, implying that the centrosome is involved in
201 both junctional adhesion and the apical-basal polarization that precedes vascular lumen
202 formation or stabilization.

203

204 Our data highlights important roles for the centrosome in maintaining junction
205 integrity and lumen development in interphase cells. Besides overduplication,
206 centrosome function can be impacted by centriole loss or structural defects. While over-
207 duplication allows for progression through the cell-cycle, mis-localization of centrosomal
208 proteins, structural deficits, and centrosome loss all result in cell-cycle arrest during G1
209 [34]. The ability to examine effects of centrosome loss on interphase cell behavior is
210 therefore compromised, highlighting the utility of a centrosome overduplication model to
211 study centrosome function.

212

213 We show that EC cell-cell junctions are disrupted downstream of centrosome
214 perturbations. It is likely that these junctional defects contribute to poor lumenization *in*
215 *vitro* and *in vivo*. EC junctions are linked to vascular lumen formation during
216 anastomosis, where VE-cadherin facilitates tip cell interactions and subsequent junction

217 rearrangements necessary to form a continuous lumen [35,36]. Moreover, genetic loss
218 of VE-cadherin in mice or zebrafish leads to lumen defects, vascular dysfunction, and
219 embryonic lethality [22,23], supporting a link between disrupted adherens junctions and
220 malformed lumens in EC sprouts.
221
222 Our results reveal that lumens are perturbed following centrosome
223 overduplication in both an *in vitro* angiogenesis model lacking physiological flow and in
224 an *in vivo* zebrafish model with blood flow. These findings indicate that lumenal defects
225 resulting from excess centrosomes do not depend on shear stress exerted by blood
226 flow. During later stages of angiogenesis, high pressure from blood flow is necessary for
227 changes in cell morphology resulting in functional lumens [37]. However, lumens can
228 also form *in vitro* and *in vivo* absent blood flow [7,38]. Hultin and colleagues showed
229 that disruption of the VE-cadherin junctional complex via the scaffolding protein amotL2
230 was sufficient to prevent lumenal expansion independent of blood flow through changes
231 in cell contractility [38]. Thus, it is likely that the profound changes in VE-cadherin
232 localization at EC cell-cell junctions following centrosome over-duplication alter the
233 ability of EC to properly coordinate the cytoskeletal forces needed for polarization and
234 lumenogenesis, regardless of blood flow.
235
236 In summary, by providing the first link between centrosome perturbation and
237 adherens junction stability and lumenization, our data indicate a novel role for the
238 centrosome in EC polarity, junctions, and lumenization in blood vessels. These
239 abnormalities may contribute to tumor blood vessel dysfunction.

240 **MATERIALS & METHODS**

241 ***Cell culture***

242 HUVEC (C2519A, Lonza) were cultured in EBM-2 (CC-3162, Lonza)
243 supplemented with the Endothelial Growth Medium (EGM-2) bullet kit (CC-3162, Lonza)
244 and 1x antibiotic-antimycotic (Gibco). Normal human lung fibroblasts (CC2512, Lonza)
245 were cultured in DMEM (Gibco) with 10% fetal bovine serum (FBS) and 1x antibiotic-
246 antimycotic (Gibco). All cells were maintained at 37°C and 5% CO_2. Tetracycline-
247 inducible Plk4-overexpression HUVEC were generated as previously described
248 [13,15,30]. Viruses were produced by the UNC Lenti-shRNA Core Facility. To induce
249 centrosome overduplication, tet-Plk4 HUVEC were treated with 1µg/ml doxycycline
250 (DOX, D9891, Sigma) for 24hr followed by washout. Experiments were performed 48hr
251 following DOX addition.

252

253 ***3D sprouting angiogenesis assay***

254 The 3D sprouting angiogenesis assay was performed as previously described
255 with the following changes [15,39]. Tet-Plk4 HUVEC were treated with 1µg/ml DOX for
256 24hr at 37°C. 13µl/ml centrin:eGFP lentivirus and 1µg/ml Polybrene were added to
257 HUVEC 16hr post DOX addition for the last 8hr of DOX treatment. Cells were washed
258 with Dulbecco's phosphate-buffered saline (DPBS) (MT-21-031-CV, Corning) and fresh
259 media was added to remove the virus and DOX. The following day, infected cells were
260 coated onto cytodex 3 microcarrier beads (17048501, GE Healthcare Life Sciences)
261 and embedded in a fibrin matrix as described. Z-stacks were acquired with an Olympus
262 confocal microscope (FV1200 or FV3000) and processed in Image J (National Institutes

263 of Health). Total vessel width was measured in the YZ plane by drawing a line through
264 the nucleus and across the entire vessel. Lumen width was measured in the YZ plane
265 using Moesin1 staining (1:1000, ab52490, Abcam) as a surrogate for the apical surface
266 and normalized to total vessel width. DAPI (10236276001, Sigma) was used to visualize
267 the nucleus.
268
269 ***Micropatterns***
270 Large H-micropatterns (CYTOO) were coated with 5µg/ml fibronectin and seeded
271 with HUVEC according to manufacturer's instructions. Cells were allowed to spread for
272 24hr, then fixed with ice-cold methanol for 10 min at 4°C.
273
274 ***Immunofluorescence and quantification***
275 Fixed HUVEC were blocked for 1hr at RT in blocking solution (5% FBS, 2X
276 antibiotic-antimycotic (Gibco), 0.1% sodium azide (s2002-100G, Sigma) in DPBS). Cells
277 were incubated in primary antibody overnight at 4°C, then washed 3X for 5 min in
278 DPBS. Secondary antibody and DRAQ7 (1:1000, ab109202, Abcam) were added for
279 1hr at RT followed by 3X washes for 10 min each in DPBS. Slides were mounted with
280 coverslips using Prolong Diamond Antifade mounting medium (P36961, Life
281 Technology) and sealed with nail polish. Primary and secondary antibodies were diluted
282 in blocking solution. Images were acquired with an Olympus confocal microscope
283 (FV1200 or FV3000) and analyzed using ImageJ. Centrosome overduplication was
284 quantified by counting centrosome number in at least 500 cells per replicate. Junction
285 area on micropatterns was quantified by thresholding the VE-cadherin staining and

286 measuring total VE-cadherin area in ImageJ. VE-cadherin distribution on doublet
287 micropatterns was measured in ImageJ by drawing a line across the junction (from
288 centrosome in first cell to centrosome in second cell) and acquiring a line scan of VE-
289 cadherin intensity. Peaks were counted for each pattern and normalized to the line
290 length. Only peaks above half of the maximum VE-cadherin intensity were counted. The
291 following primary antibodies were used: anti-γ-tubulin (1:5000, T6557, Sigma-Aldrich),
292 anti-VE-cadherin (1:500, 2500S, Cell Signaling), anti-Moesin-1 (1:1000, ab52490,
293 Abcam). The following secondary antibodies from Thermo Fisher Scientific were used:
294 goat anti-mouse AlexaFluor 488 (1:500, A11029), goat anti-mouse AlexaFluor 594
295 (1:500, A11005), goat anti-rabbit AlexaFluor 488 (1:500, A11034), goat anti-rabbit
296 AlexaFluor 594 (1:500, A11037).
297
298 ***Zebrafish***
299 Zebrafish (*Danio rerio*) were housed in an institutional animal care and use
300 committee (IACUC)-approved facility. Zebrafish were maintained as previously
301 described (Wiley, *et al*., 2011). *Tg(kdrl:mCherry)* was a gift from D. Stainier.
302 *Tg(fli:centrin-GFP*) was created by subcloning centrin:GFP into the pCR8/GW/TOPO
303 middle entry vector (Thermo Fisher) and then gateway cloning into the pDestTol2CG2
304 plasmid (REF Tol2 kit). Tol2 transposase RNA was generated using the sp6 mMessage
305 mMachine synthesis kit (AM1340, Thermo Fisher). For overexpression of *Plk4*, *p2a-*
306 *Lox-mCherry-STOP-Lox-Plk4* was fused to the 3' end of the endogenous *kdrl* gene. The
307 assembled construct was subcloned into the pKHR4 backbone and linearized by IsceI
308 digest. 200ng/µl sgRNA (5'-*TCTGGTTTGGAAGGACACAG*-3') and 700ng/µl of Cas9

309 recombinant protein (PNABio) were injected into one-cell stage *tg(fli:centrin-GFP)*
310 embryos alongside the construct to generate double stranded breaks at the 3' end of
311 the *kdrl* gene and induce homologous recombination as previous described [40]. F1
312 were injected with Cre mRNA at the 1-2 cell stage. Cre mRNA was obtained by
313 subcloning the *Cre* gene from the pME-ERT2-Cre-ERT2 plasmid into the
314 pCR8/GW/TOPO middle entry vector, gateway cloning into a pCS Dest vector, then
315 preparing RNA with the sp6 mMessageMachine synthesis kit. pME-ERT2-Cre-ERT2
316 was a gift from Kryn Stankunas (Addgene plasmid # 82587;
317 http://n2t.net/addgene:82587; RRID:Addgene 82587). Embryos were collected from
318 desired crosses and grown in E3 at 28.5°C. At 72 hpf, embryos were injected with
319 Qdot605 (Q10103MP, Thermo Fisher). Fish were fixed by incubating dechorionated
320 embryos in ice cold 4% PFA at 4°C overnight. Embryos were rinsed in PBS and
321 mounted using a fine probe to de-yolk and a small blade to separate the trunk from the
322 cephalic region and using VECTASHIELD® Hardset™ Antifade Mounting Medium. The
323 coverslip was sealed with petroleum jelly before imaging on an Olympus FV1200
324 confocal microscope. Centrosome overduplication was confirmed in Plk4-
325 overexpressing embryos based on centrin-GFP centriole labeling. ISV perfusion was
326 measured by counting the number of perfused ISVs based on Qdot605 signal as a
327 percentage of total ISV number (visualized using *Tg(kdrl:mCherry)*).
328
329 ***Statistics***
330 Student's two-tailed *t* test was used to determine statistical significance in
331 experiments with 2 groups. One-way ANOVA with Tukey's multiple comparisons test

332 was used to determine statistical significance for experiments with 3 groups, and X^2 or
333 two-way ANOVA with Sidak's correction were used for categorical data. Error bars
334 represent the mean ± standard deviation. Statistical tests and graphs were made using
335 the Prism 7 software (GraphPad Software).
336

337 **ACKNOWLEGMENTS**

338 We thank Tony Perdue and the UNC Biology Microscopy Core, the UNC Lenti-
339 shRNA Core, Maryanna Parker and Allison Marvin for fish room support, and Bautch lab
340 members for critical discussions.
341

342 **FUNDING**

343 This work was supported by grants from the National Institutes of Health
344 (HL43174, HL116719, HL117256, HL139950 to VLB), a K99/R00 (1K99HL124311-
345 01A1 to EJK), the Integrated Vascular Biology Training Grant (5T32HL069768-17 to
346 DMB), and an American Heart Association Predoctoral Fellowship (19PRE34380887 to
347 DMB).
348

349 **DECLARATION OF INTERESTS:** None.
350
351

352 **REFERENCES**

353 1. Carmeliet P, Jain RK. (2011) Molecular mechanisms and clinical applications of
354 angiogenesis. Nature. 2011;473(7347):298–307.
355 2. Bautch VL, Caron KM. (2015) Blood and lymphatic vessel formation. Cold Spring
356 Harb Perspect Biol. 2015;7(3):a008268.
357 3. Kushner E, Bautch V. (2013) Building blood vessels in development and disease.
358 Curr Opin Hematol. 2013;20(3):231–6.
359 4. Blum Y, Belting HG, Ellertsdottir E, Herwig L, Luders F, Affolter M. (2008)
360 Complex cell rearrangements during intersegmental vessel sprouting and vessel
361 fusion in the zebrafish embryo. Dev Biol. 2008;316:312–22.
362 5. Iruela-Arispe ML, Davis GE. (2009) Cellular and molecular mechanisms of
363 vascular lumen formation. Dev Cell. 2009;16(2):222–31.
364 6. Strilic B, Kucera T, Eglinger J, Hughes MR, McNagny KM, Tsukita S, et al. (2009)
365 The molecular basis of vascular lumen formation in the developing mouse aorta.
366 Dev Cell. 2009;17(4):505–15.
367 7. Wang Y, Kaiser MS, Larson JD, Nasevicius A, Clark KJ, Wadman SA, et al.
368 (2010) Moesin1 and VE-cadherin are required in endothelial cells during in vivo
369 tubulogenesis. Development. 2010;137(18):3119–28.
370 8. Lee CY, Bautch VL. (2011) Ups and downs of guided vessel sprouting: the role of
371 polarity. Physiology. 2011;26(5):326–33.
372 9. Pelton JC, Wright CE, Leitges M, Bautch VL. (2014) Multiple endothelial cells
373 constitute the tip of developing blood vessels and polarize to promote lumen
374 formation. Development. 2014;141(21):4121–6.

375 10. Aird WC. (2012) Endothelial cell heterogeneity. Cold Spring Harb Perspect Med.
376 2012;2(1):a006429.
377 11. Hashizume H, Baluk P, Morikawa S, McLean JW, Thurston G, Roberge S, et al.
378 (2000) Openings between defective endothelial cells explain tumor vessel
379 leakiness. Am J Pathol. 2000;156(4):1363–80.
380 12. Carmeliet P, Jain RK. (2011) Principles and mechanisms of vessel normalization
381 for cancer and other angiogenic diseases. Nat Rev Drug Discov. 2011;10:417–27.
382 13. Kushner EJ, Ferro LS, Liu J-Y, Durrant JR, Rogers SL, Dudley AC, et al. (2014)
383 Excess centrosomes disrupt endothelial migration via centrosome scattering. J
384 Cell Biol. 2014;206(2):257–72.
385 14. Hida K, Hida Y, Amin DN, Flint AF, Panigrahy D, Morton CC, et al. (2004) Tumor-
386 Associated Endothelial Cells with Cytogenetic Abnormalities. Cancer Res.
387 2004;64(22):8249–55.
388 15. Kushner EJ, Ferro LS, Yu Z, Bautch VL. (2016) Excess centrosomes perturb
389 dynamic endothelial cell repolarization during blood vessel formation. Mol Biol
390 Cell. 2016;27(12):1911–20.
391 16. Godinho SA, Picone R, Burute M, Dagher R, Su Y, Leung CT, et al. (2014)
392 Oncogene-like induction of cellular invasion from centrosome amplification.
393 Nature. 2014;510(7503):167–71.
394 17. Taylor SM, Nevis KR, Park HL, Rogers GC, Rogers SL, Cook JG, et al. (2010)
395 Angiogenic factor signaling regulates centrosome duplication in endothelial cells
396 of developing blood vessels. Blood. 2010;116(16):3108–17.
397 18. Komarova YA, Huang F, Geyer M, Daneshjou N, Garcia A, Idalino L, et al. (2012)

398 VE-cadherin signaling induces EB3 phosphorylation to suppress microtubule
399 growth and assemble adherens junctions. Mol Cell. 2012;48(6):914–25.
400 19. Phng L-K, Gebala V, Bentley K, Philippides A, Wacker A, Mathivet T, et al. (2015)
401 Formin-mediated actin polymerization at endothelial junctions is required for
402 vessel lumen formation and stabilization. Dev Cell. 2015;32(1):123–32.
403 20. Spracklen AJ, Peifer M. (2015) Actin and apical constriction: some (re)-assembly
404 required. Dev Cell. 2015;35(6):662–4.
405 21. Nowotarski SH, Peifer M. (2014) Cell biology: a tense but good day for actin at
406 cell-cell junctions. Curr Biol. 2014;24(15):R688–90.
407 22. Carmeliet P, Lampugnani M-G, Moons L, Breviario F, Compernolle V, Bono F, et
408 al. (1999) Targeted deficiency or cytosolic truncation of the VE-cadherin gene in
409 mice impairs VEGF-mediated endothelial survival and angiogenesis. Cell.
410 1999;98(2):147–57.
411 23. Montero-Balaguer M, Swirsding K, Orsenigo F, Cotelli F, Mione M, Dejana E.
412 (2009) Stable vascular connections and remodeling require full expression of VE-
413 cadherin in zebrafish embryos. PLoS One. 2009;4(6):e5772.
414 24. Kollman JM, Merdes A, Mourey L, Agard DA. (2011) Microtubule nucleations by
415 gamma-tubulin complexes. Nat Rev Mol Cell Biol. 2011;12:709–21.
416 25. Bettencourt-Dias M, Glover DM. (2007) Centrosome biogenesis and function:
417 centrosomics brings new understanding. Nat Rev Mol Cell Biol. 2007;8:451–63.
418 26. Pelaseyed T, Bretscher A. (2018) Regulation of actin-based apical structures on
419 epithelial cells. J Cell Sci. 2018;131:jcs221853.
420 27. Wu S-Z, Bezanilla M. (2018) Actin and microtubule cross talk mediates persistent

421 polarized growth. J Cell Biol. 2018;217(10):3531.
422 28. St Johnston D, Sanson B. (2011) Epithelial polarity and morphogenesis. Curr
423 Opin Cell Biol. 2011;23(5):540–6.
424 29. Habedanck R, Stierhof YD, Wilkinson CJ, Nigg EA. (2005) The Polo kinase Plk4
425 functions in centriole duplication. Nat Cell Biol. 2005;7(11):1140–6.
426 30. Yu Z, Ruter DL, Kushner EJ, Bautch VL. (2017) Excess centrosomes induce p53-
427 dependent senescence without DNA damage in endothelial cells. FASEB J.
428 2017;10:4295–304.
429 31. Iden S, Rehder D, August B, Suzuki A, Wolburg-Buchholz K, Wolburg H, et al.
430 (2006) A distinct PAR complex associates physically with VE-cadherin in
431 vertebrate endothelial cells. EMBO Rep. 2006;7(12):1239–46.
432 32. Bentley K, Franco CA, Philippides A, Blanco R, Dierkes M, Gebala V, et al. (2014)
433 The role of differential VE-cadherin dynamics in cell rearrangement during
434 angiogenesis. Nat Cell Biol. 2014;16(4):309–21.
435 33. Lampugnani M-G, Orsenigo F, Rudini N, Maddaluno L, Boulday G, Chapon F, et
436 al. (2010) CCM1 regulates vascular-lumen organization by inducing endothelial
437 polarity. J Cell Sci. 2010;123:1073–80.
438 34. Mikule K, Delaval B, Kaldis P, Jurcyzk A, Hergert P, Doxsey S. (2007) Loss of
439 centrosome integrity induces p38-p53-p21-dependent G1-S arrest. Nat Cell Biol.
440 2007;9:160–70.
441 35. Lenard A, Ellertsdottir E, Herwig L, Krudewig A, Sauteur L, Belting H-G, et al.
442 (2013) In vivo analysis reveals a highly stereotypic morphogenetic pathway of
443 vascular anastomosis. Dev Cell. 2013;25(5):492–506.

444 36. Herwig L, Blum Y, Krudewig A, Ellertsdottir E, Lenard A, Belting H-G, et al. (2011)
445 Distinct cellular mechanisms of blood vessel fusion in the zebrafish embryo. Curr
446 Biol. 2011;21(22):1942–8.
447 37. Gebala V, Collins R, Geudens I, Phng L-K, Gerhardt H. (2016) Blood flow drives
448 lumen formation by inverse membrane blebbing during angiogenesis in vivo. Nat
449 Cell Biol. 2016;18(4):443–50.
450 38. Hultin S, Zheng Y, Mahdi M, Vertuani S, Gentili C, Balland M, et al. (2014)
451 AmotL2 links VE-cadherin to contractile actin fibres necessary for aortic lumen
452 expansion. Nat Commun. 2014;5:3743.
453 39. Nakatsu MN, Hughes CCW. (2008) An optimized three-dimensional in vitro model
454 for the analysis of angiogenesis. Methods Enzymol. 2008;443:65–82.
455 40. Hoshijima K, Jurynec MJ, Grunwald DJ. (2016) Precise editing of the zebrafish
456 genome made simple and efficient. Dev Cell. 2016;36(6):654–67.
457

458 **FIGURE LEGENDS**

459 **Figure 1. Excess centrosomes perturb polarity between EC sharing junctions.**

460 **(a)** Schematic of *Plk4* overexpression in HUVEC. TRE, tet-responsive element; rtTA,

461 reverse tet transactivator **(b)** Schematic of H-micropattern with possible centrosome

462 positions. **(c)** Representative images of EC on H-micropatterns with either 1-2

463 centrosomes (left) or more than 2 centrosomes (right). Yellow arrowheads, normal

464 centrosomes with distal localization. White arrowheads, over-duplicated centrosomes

465 with proximal (top cell) and central (bottom cell) localization. Insets show centrosome

466 number. Scale bar, 10μm. **(d)** Quantification of EC centrosome position. Significance of

467 proximal location for 1-2 centrosomes vs. >2 centrosomes by two-way ANOVA with

468 Sidak's correction. **, $p \leq 0.01$. **(e)** Quantification of polarity pattern. **(f)** Quantification of

469 polarity mismatch. N=4 replicates. Statistics: χ^2 analysis unless otherwise stated. (N:N),

470 both EC 1-2 centrosomes/cell; (O:O), both EC >2 centrosomes/cell.

471

472 **Figure 2. EC with excess centrosomes form disorganized adherens junctions.**

473 **(a-a'')** Schematics showing potential arrangements of EC on H-patterns. **(b-b'')**

474 Representative images of cell-cell junctions on H patterns with EC centrosome status

475 N:N (**b**), N:O (**b'**), or O:O (**b''**). EC were stained for γ-tubulin (green), VE-cadherin (red),

476 and DNA (blue, DRAQ7). Scale bar, 10μm. **(c-c'')** Representative line scans of VE-

477 cadherin signal between centrosomes in N:N (**c**), N:O (**c'**), or O:O (**c''**) EC junctions. #,

478 positive peak. **(d)** Quantification of VE-cadherin area in EC junctions with the indicated

479 centrosome complements. **(e)** Quantification of peaks/length of VE-cadherin line scans

480 of EC junctions with indicated centrosome complements. N=4 replicates. Statistics: one-
481 way ANOVA with Tukey's correction. *, $p \leq 0.05$, **, $p \leq 0.01$, ***, $p \leq 0.001$, ****, $p \leq 0.0001$.
482
483 **Figure 3. Sprouts containing EC with excess centrosomes have abnormal**
484 **lumens.**
485 **(a)** Schematic showing the XY plane of a vessel sprout and indicating centrosome
486 position scoring criteria. **(b)** epresentative images showing lumen diameter in EC with
487 indicated centrosome number. Left panels, XY axis; right panels, YZ axis. Centrin::GFP
488 (green, centrosomes), Moesin1 (red, apical), DNA (cyan, DAPI). Insets show
489 centrosome number. Scale bar, 10μm. **(c)** Apical-basal centrosome position in sprouting
490 EC with indicated centrosome number. N=3 replicates. Statistics: χ^2 analysis. **(d)**
491 Moesin1 staining pattern in EC with indicated centrosome numbers. N=3 replicates.
492 Statistics: X^2 analysis. **(e)** Quantification of lumen diameter in EC with indicated
493 centrosome number. N=3 replicates. Statistics: one-way ANOVA with Tukey's
494 correction. **, $p \leq 0.01$.
495
496 **Figure 4. *Plk4* overexpression in zebrafish results in fewer lumenized vessels.**
497 **(a)** Schematic for Cre mediated overexpression of *Plk4* in zebrafish embryos. **(b)**
498 Representative image of *Plk4* overexpression in 72 hpf zebrafish embryo. tg(Fli:Centrin-
499 GFP) (green), Qdot605 (purple). Yellow arrowheads, centrosomes in EC. Scale bar, 20
500 μm. **(c)** Quantification of EC with >2 centrosomes in zebrafish with indicated
501 genotypes/conditions (WT + Cre, n=17; LSL-Plk4 uninjected, n=15; LSL-Plk4 + Cre,
502 n=14). Statistics: one-way ANOVA with Tukey's correction. ****, $p \leq 0.0001$. **(d-d'')**

503 representative images of zebrafish tails at 72 hpf perfused with Qdot605 to assess
504 lumen formation in embryos of indicated genotype and indicated injection with Cre.
505 DLAV, dorsal longitudinal anastomotic vessel; ISV, intersegmental vessel; CVP, caudal
506 vein plexus; LSL, lox-STOP-lox. **(e)** Quantification of ISV perfusion in 72 hpf embryos
507 with indicated gentoypes/condition (WT + Cre, n=5; LSL-Plk4 uninjected, n=31; LSL-
508 Plk4 + Cre, n=28). Statistics: one-way ANOVA with Tukey's correction. *, $p \leq 0.05$, ****,
509 $p \leq 0.0001$.
510

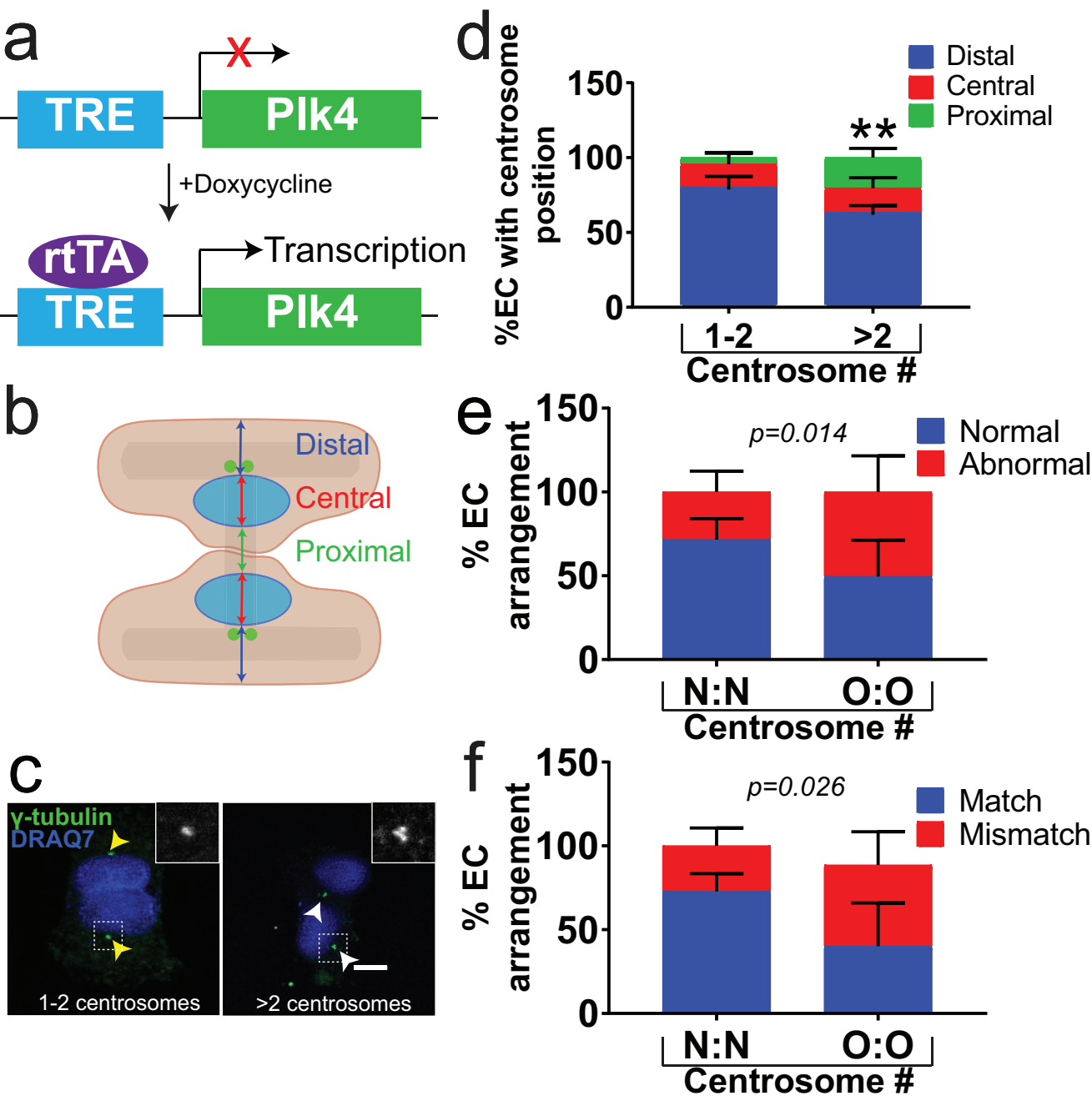
a
TRE
Plk4
+Doxycycline
rtTA
TRE
Transcription
Plk4
b
Distal
Central
Proximal
c
γ-tubulin
DRAQ7
1-2 centrosomes
>2 centrosomes
d
%EC with centrosome position
150
100
50
0
Distal
Central
Proximal
**
1-2
>2
Centrosome #
e
% EC arrangement
150
100
50
0
p=0.014
Normal
Abnormal
N:N
O:O
Centrosome #
f
% EC arrangement
150
100
50
0
p=0.026
Match
Mismatch
N:N
O:O
Centrosome #

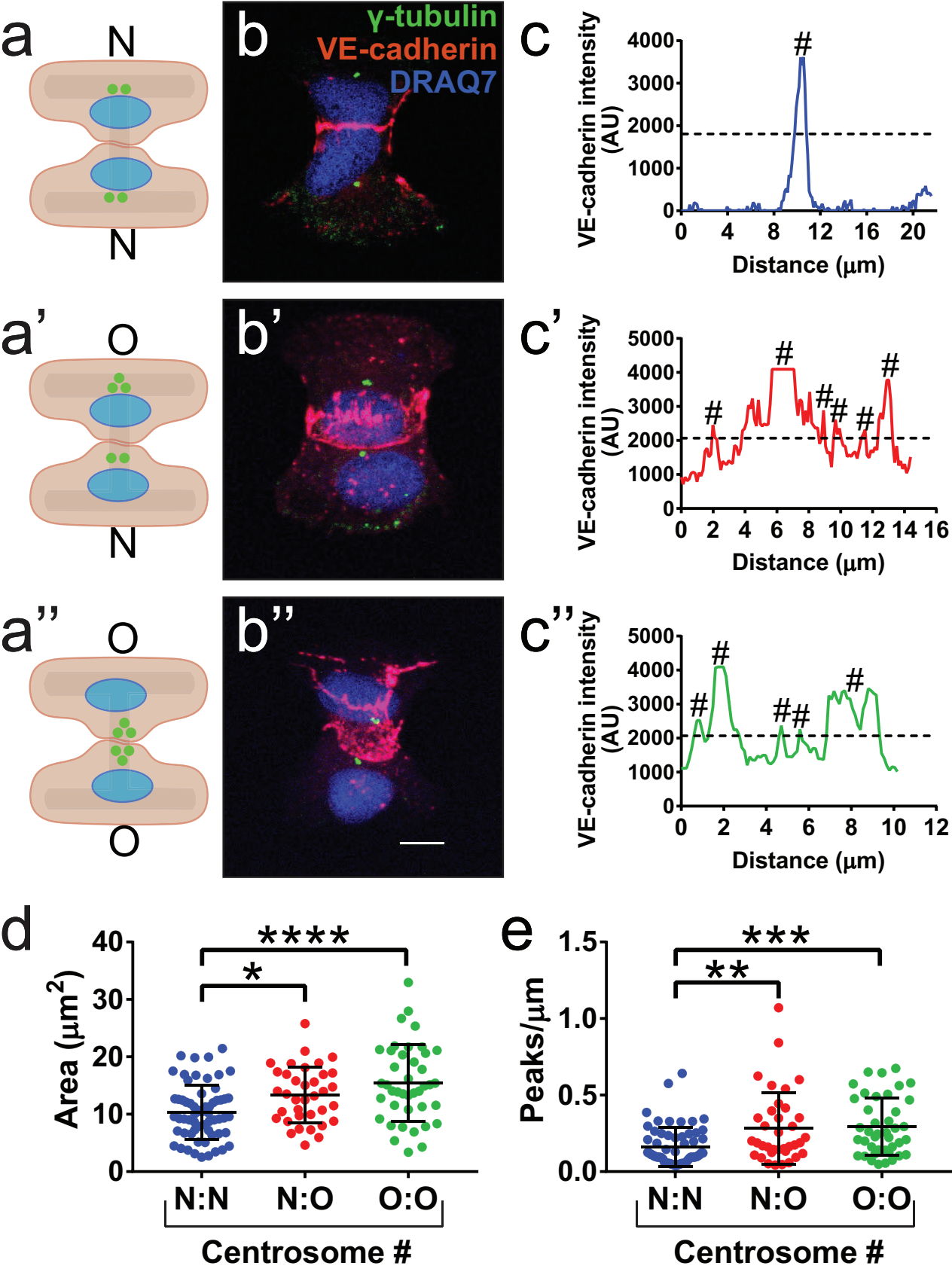
a
N
N
b
γ-tubulin
VE-cadherin
DRAQ7
c
VE-cadherin intensity (AU)
Distance (μm)
a'
O
N
b'
c'
a''
O
O
b''
c''
d
Area (μm²)
N:N
N:O
O:O
Centrosome #
e
Peaks/μm
N:N
N:O
O:O
Centrosome #

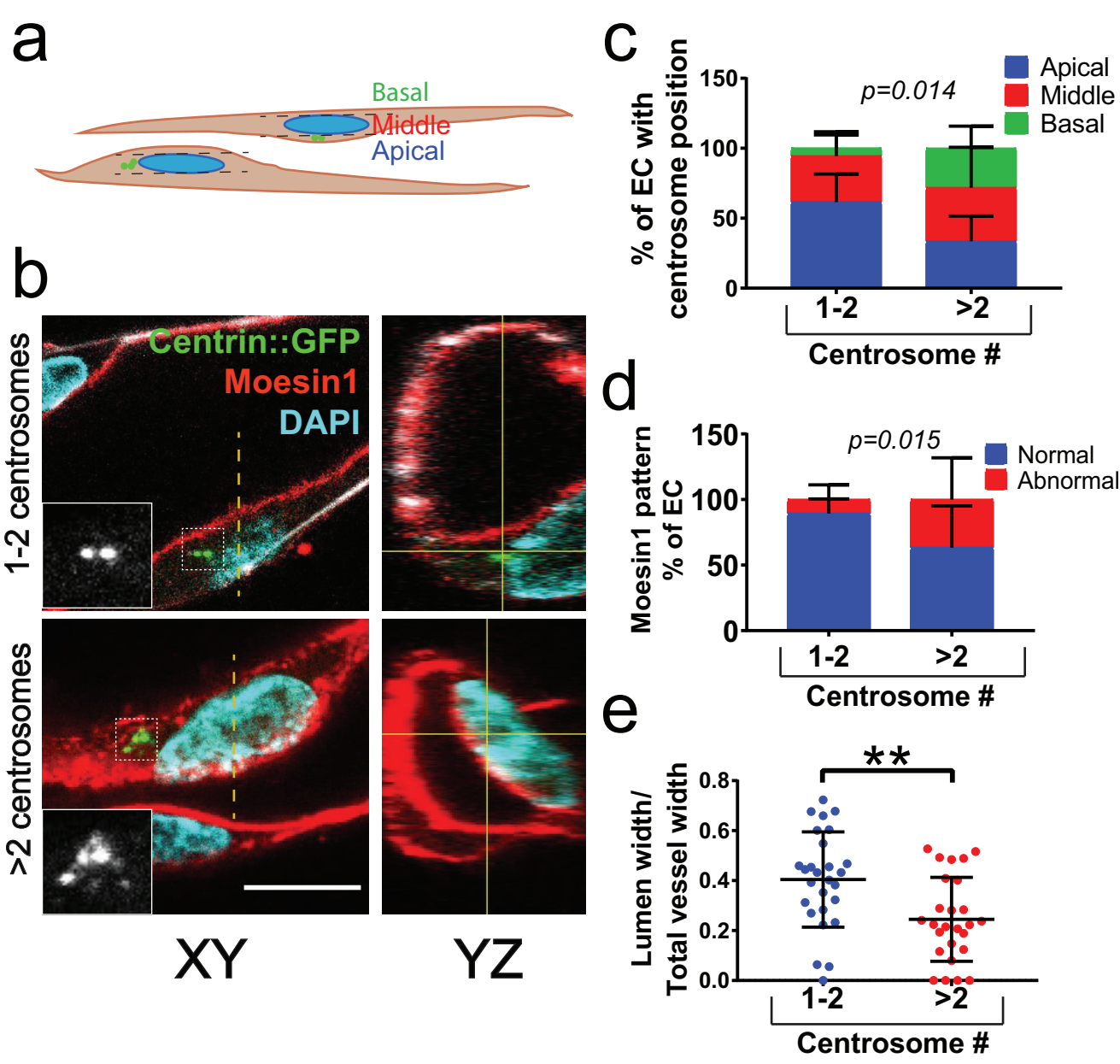
a
Basal
Middle
Apical
b
Centrin::GFP
Moesin1
DAPI
1-2 centrosomes
>2 centrosomes
XY
YZ
c
% of EC with centrosome position
150
100
50
0
p=0.014
Apical
Middle
Basal
1-2
>2
Centrosome #
d
Moesin1 pattern % of EC
150
100
50
0
p=0.015
Normal
Abnormal
1-2
>2
Centrosome #
e
Lumen width/ Total vessel width
0.8
0.6
0.4
0.2
0.0
**
1-2
>2
Centrosome #

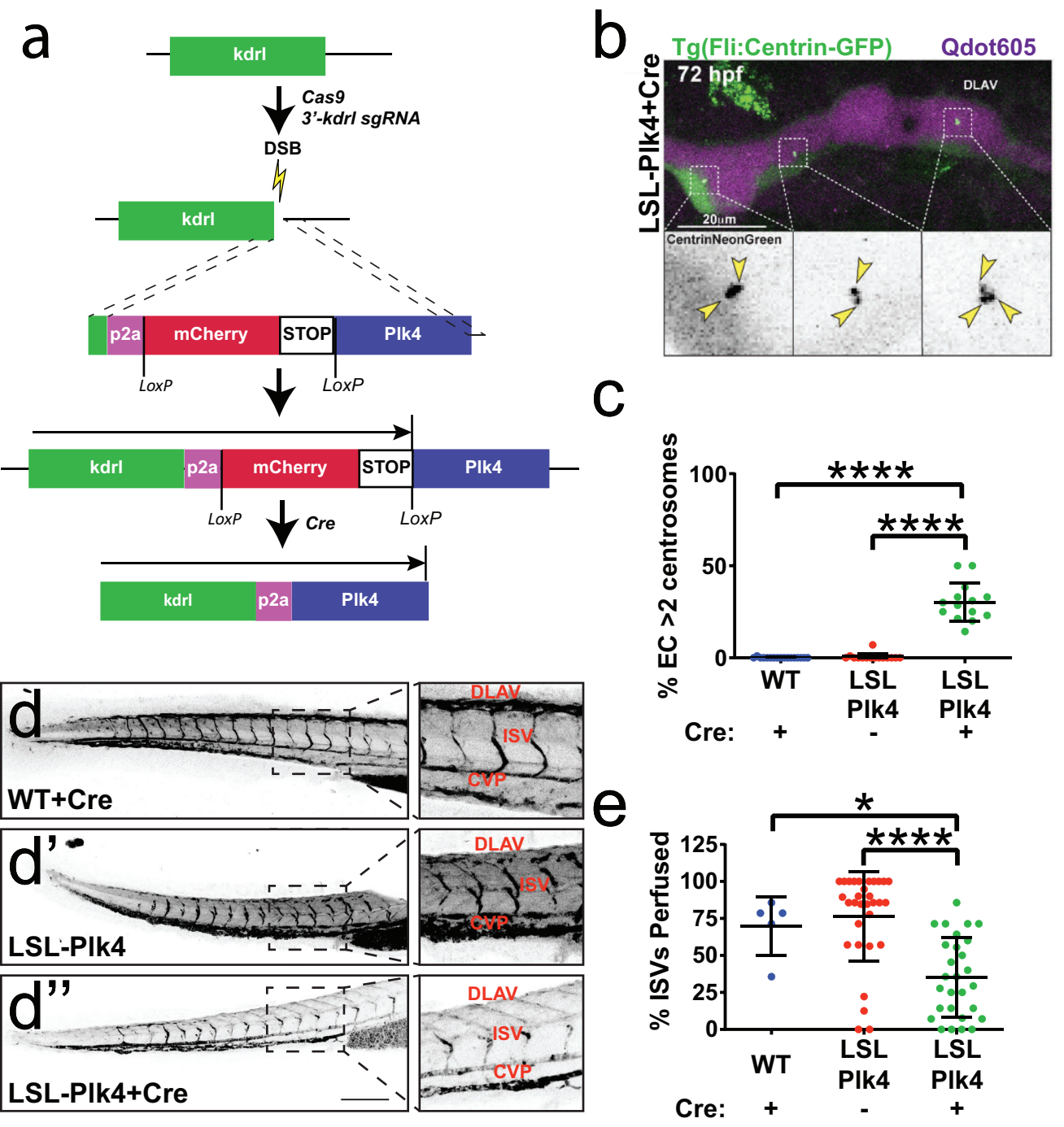
a
kdrl
Cas9
3'-kdrl sgRNA
DSB
kdrl
p2a
mCherry
STOP
Plk4
LoxP
LoxP
kdrl
p2a
mCherry
STOP
Plk4
LoxP
Cre
LoxP
kdrl
p2a
Plk4
b
Tg(Fli:Centrin-GFP)
Qdot605
LSL-Plk4+Cre
72 hpf
DLAV
20µm
CentrinNeonGreen
c
% EC >2 centrosomes
100
50
0
****
****
WT
LSL Plk4
LSL Plk4
Cre:
+
-
+
d
WT+Cre
DLAV
ISV
CVP
d'
LSL-Plk4
DLAV
ISV
CVP
d''
LSL-Plk4+Cre
DLAV
ISV
CVP
e
% ISVs Perfused
125
100
75
50
25
0
*
****
WT
LSL Plk4
LSL Plk4
Cre:
+
-
+